UNIVERSITÄT AUGSBURG
Universitätsbibliothek

OPEN ACCESS
OPUS AUGSBURG

Spatio-temporal soil moisture patterns –a meta-analysis using plot to catchment scale data

W. Korres, T. G. Reichenau, Peter Fiener, C. N. Koyama, H. R. Bogena, T. Cornelissen, R. Baatz, M. Herbst, B. Diekkrüger, Harry Vereecken, K. Schneider

Angaben zur Veröffentlichung / Publication details:

Korres, W., T. G. Reichenau, Peter Fiener, C. N. Koyama, H. R. Bogena, T. Cornelissen, R. Baatz, et al. 2015. "Spatio-temporal soil moisture patterns –a meta-analysis using plot to catchment scale data." *Journal of Hydrology* 520: 326–41. https://doi.org/10.1016/j.jhydrol.2014.11.042.

Nutzungsbedingungen / Terms of use: **CC BY-NC-ND 4.0**

Dieses Dokument wird unter folgenden Bedingungen zur Verfügung gestellt: / This document is made available under these conditions:
CC-BY-NC-ND 4.0: Creative Commons: Namensnennung - Nicht kommerziell - Keine Bearbeitung
Weitere Informationen finden Sie unter: / For more information see:
https://creativecommons.org/licenses/by-nc-nd/4.0/deed.de

Journal of Hydrology 520 (2015) 326–341

Contents lists available at ScienceDirect

Journal of Hydrology

journal homepage: www.elsevier.com/locate/jhydrol

Spatio-temporal soil moisture patterns – A meta-analysis using plot to catchment scale data

W. Korres [a,*], T.G. Reichenau [a], P. Fiener [b], C.N. Koyama [c], H.R. Bogena [d], T. Cornelissen [e], R. Baatz [d], M. Herbst [d], B. Diekkrüger [e], H. Vereecken [d], K. Schneider [a]

[a] Institute of Geography, University of Cologne, Cologne, Germany
[b] Institut für Geographie, Universität Augsburg, Augsburg, Germany
[c] Center for Northeast Asian Studies, Division of Geoscience and Remote Sensing, Tohoku University, Sendai, Japan
[d] Agrosphere Institute, IBG-3, Forschungszentrum Jülich, Jülich, Germany
[e] Department of Geography, University of Bonn, Bonn, Germany

ARTICLE INFO

Article history:
Received 8 September 2014
Received in revised form 7 November 2014
Accepted 13 November 2014
Available online 21 November 2014
This manuscript was handled by Corrado Corradini, Editor-in-Chief

Keywords:
Catchment hydrology
Soil moisture
Patterns
Scale
Geostatistics
Fractal analysis

SUMMARY

Soil moisture is a key variable in hydrology, meteorology and agriculture. It is influenced by many factors, such as topography, soil properties, vegetation type, management, and meteorological conditions. The role of these factors in controlling the spatial patterns and temporal dynamics is often not well known. The aim of the current study is to analyze spatio-temporal soil moisture patterns acquired across a variety of land use types, on different spatial scales (plot to meso-scale catchment) and with different methods (point measurements, remote sensing, and modeling). We apply a uniform set of tools to determine method specific effects, as well as site and scale specific controlling factors. Spatial patterns of soil moisture and their temporal development were analyzed using nine different datasets from the Rur catchment in Western Germany. For all datasets we found negative linear relationships between the coefficient of variation and the mean soil moisture, indicating lower spatial variability at higher mean soil moisture. For a forest sub-catchment compared to cropped areas, the offset of this relationship was larger, with generally larger variability at similar mean soil moisture values. Using a geostatistical analysis of the soil moisture patterns we identified three groups of datasets with similar values for sill and range of the theoretical variogram: (i) modeled and measured datasets from the forest sub-catchment (patterns mainly influenced by soil properties and topography), (ii) remotely sensed datasets from the cropped part of the Rur catchment (patterns mainly influenced by the land-use structure of the cropped area), and (iii) modeled datasets from the cropped part of the Rur catchment (patterns mainly influenced by large scale variability of soil properties). A fractal analysis revealed that all analyzed soil moisture patterns showed a multifractal behavior, with at least one scale break and generally high fractal dimensions. Corresponding scale breaks were found between different datasets. The factors causing these scale breaks are consistent with the findings of the geostatistical analysis. Furthermore, the joined analysis of the different datasets showed that small differences in soil moisture dynamics, especially at the upper and lower bounds of soil moisture (at maximum porosity and wilting point of the soils) can have a large influence on the soil moisture patterns and their autocorrelation structure. Depending on the prevalent type of land use and the time of year, vegetation causes a decrease or an increase of spatial variability in the soil moisture pattern.

© 2014 The Authors. Published by Elsevier B.V. This is an open access article under the CC BY-NC-ND license (http://creativecommons.org/licenses/by-nc-nd/3.0/).

1. Introduction

Soil moisture is a key variable in hydrology, meteorology and agriculture. Its spatial patterns and temporal dynamics are controlled by many factors, such as topography, soil properties, vegetation type, solar radiation, management, and precipitation (Famiglietti et al., 1998; Hawley et al., 1983; Hebrard et al., 2006; Korres et al., 2010; Rodriguez-Iturbe et al., 2006; Rosenbaum et al., 2012; Svetlitchnyi et al., 2003; Western et al., 1998, 1999a). Reynolds (1970) distinguished between static (e.g., soil texture, topography) and dynamic (e.g., precipitation, vegetation) factors affecting soil moisture at a given location. Grayson et al. (1997) attributed controlling factors to two different soil moisture states. The wet state is not controlled locally and is dominated by non-local lateral fluxes, while the dry state is dominated

* Corresponding author. Tel.: +49 221 470 7802; fax: +49 221 470 5124.
E-mail address: wolfgang.korres@uni-koeln.de (W. Korres).

http://dx.doi.org/10.1016/j.jhydrol.2014.11.042
0022-1694/© 2014 The Authors. Published by Elsevier B.V.
This is an open access article under the CC BY-NC-ND license (http://creativecommons.org/licenses/by-nc-nd/3.0/).

by vertical water fluxes at a given location. Generally, the approach by Grayson et al. (1997) underlines the importance of temporal dynamics for the development of soil moisture patterns.

During the last decades, great efforts were undertaken to understand soil moisture dynamics in a spatial context, and to determine controlling factors and scaling properties (Corradini, 2014). Datasets derived on different spatial scales were utilized in the past, ranging from point measurements at the plot scale to small catchments (e.g. Bogena et al., 2010; Famiglietti et al., 1998; Western et al., 1998) and from remote sensing based data (e.g. Kim and Barros, 2002; Koyama et al., 2010; Montzka et al., 2013; Rodriguez-Iturbe et al., 1995) to modeled soil moisture data (e.g. Herbst and Diekkruger, 2003; Korres et al., 2013; Manfreda et al., 2007; Peters-Lidard et al., 2001) at the small scale to meso-scale catchments.

The results reported for the relationship between soil moisture variability and mean soil moisture are in part controversial. For the relationship between mean soil moisture and the coefficient of variation most studies found an increase in spatial variability with decreasing mean soil moisture (Choi and Jacobs, 2011; Famiglietti et al., 1999; Hu et al., 2011; Korres et al., 2013; Koyama et al., 2010). Regarding the relationship between the mean soil moisture and the standard deviation many studies reported a convex shape with a peak in variability in the intermediate soil moisture state (Choi and Jacobs, 2007; Lawrence and Hornberger, 2007; Rosenbaum et al., 2012; Ryu and Famiglietti, 2005), others found a more linear trend with an increasing variance with increasing mean soil moisture (Famiglietti et al., 1998; Western and Grayson, 1998) or no systematic trend (Yoo and Kim, 2004). Teuling and Troch (2005) showed that both soil properties and vegetation dynamics can act to either create or destroy spatial variability, depending on whether or not the soil dries below stressed conditions for transpiration. Rodriguez-Iturbe et al. (1995) and Manfreda et al. (2007) showed that soil moisture variability not only depends on mean soil moisture, but also varies with the spatial scale of the analysis.

Autocorrelation length is often used to analyze the spatial structure of soil moisture patterns. Western et al. (1998) found shorter autocorrelation lengths on wet days in a small grassland catchment, related to the smaller spatial scale of lateral redistribution, in contrast to longer autocorrelation lengths on dry dates, connected to the larger scale of evapotranspiration as the dominant factor. Also Hu et al. (2011) found a negative correlation between autocorrelation length and mean soil moisture on a 100 m grassland transect. At the field scale (mainly on wheat fields) in a semi-arid climate, Green and Erskine (2004) found spatial structures of surface soil moisture, but no clear connection of the autocorrelation length to dry or wet soil moisture conditions. Western et al. (2004) compared soil moisture autocorrelation lengths and terrain attributes, indicating the important role of topography at one site and the variation of soil properties at other sites. For a catchment with heterogeneous agricultural use, Korres et al. (2013) found that shorter autocorrelation lengths within the growing period of different crops are caused by land use patterns, i.e. varying transpiration rates of different crops. Outside of the growing period the longer autocorrelation lengths were mainly caused by large scale patterns of soil properties.

When analyzing different datasets, it is of great importance to take the influence of varying scales between these datasets into account. According to Blöschl and Sivapalan (1995) the organization of measurements (or model results) can be generally characterized by three types of scales: spacing, extent, and support. Spacing refers to the distance (or time) between the measurements, extent to the overall coverage of the measurements (in time or space), and support to the averaging volume or area (or time) of a single measurement. If the spacing is too large, small scale variability will not be captured. If the extent is too small, large scale variability will not be captured and if the support is too large, variability will be smoothed out (Grayson and Blöschl, 2000). Thus, ideally the scale of a process equals the scale of a measurement (equals the scale of a model), respectively.

Better understanding of scale dependent processes is needed (i) to optimize the efficiency of field investigations (ii) to improve the resulting interpolation by customizing the sampling scheme (Burrough, 1983) and (iii) for the transformation of point-scale measurements and parameterizations to scales required for climate studies, operational weather forecasting, and large scale hydrological modeling (Teuling and Troch, 2005).

For the current study we analyzed measured and modeled spatio-temporal soil moisture patterns for the Rur catchment using different datasets from the plot to the whole catchment scale. These datasets were acquired using different methods at locations with diverse land use. The primary aim of this meta-analysis is to overcome the difficulties in generalizing partly contradictory results associated with individual studies. Therefore it is intended (i) to compile a consistent dataset representing soil moisture data acquired on different scales (plot to meso-scale catchment) and with different methods (point measurements, remote sensing, and modeling) and (ii) to analyze the different datasets with one set of tools which should allow to determine method specific effects and site and scale specific controlling factors.

2. Materials and methods

2.1. Data sets

All datasets used in this meta-analysis were acquired within the Rur catchment, which is located at the western border of Germany, with small parts in Belgium and the Netherlands (Fig. 1). The Rur catchment is the central investigation area of the Collaborative Research Center SFB/TR 32 (Vereecken et al., 2010) and part of the Terrestrial Environmental Observatories (TERENO) infrastructure (Zacharias et al., 2011). The catchment covers a total area of 2364 km^2 and can be subdivided into two major landscape units: (i) The southern part (approx. 1260 km^2) is a low mountain range with forest and grassland characterized by a rolling topography, a mean elevation of about 690 m above sea level and a mean annual precipitation of about 1400 mm. The major soils are Fluvisols, Gleysols (along the Rur and its tributaries), Eutric Cambisols and Stagnic Gleysols with a silt loam texture (all soils in FAO soil classification). (ii) The northern part of the Rur catchment (approx. 1100 km^2) is dominated by arable land (46% of the area). The area is located in the Belgium–Germany loess belt, where crops are grown on a virtually flat terrain (slopes less than 4°). The main crops are winter cereals (mainly winter wheat), sugar beet and maize. The fertile loess plain has a mean elevation of about 100 m above sea level and a mean annual precipitation of about 700 mm. The major soils are Cumulic Anthrosols near the drainage lines and Haplic Luvisols, both with silt loam textures. Soils with a loamy sand texture (Fimic Anthrosols and Dystric Cambisols) are located on the northernmost part of the loess plain. Soils close to the Rur are Gleysols and Fluvisols with silty loam and loamy sand textures. A summary of all datasets can be found in Table 1.

2.1.1. Plot scale

A bare soil test plot (50°52′9″N, 6°27′0″E) was located 6 km southeast of the Research Center Jülich, within the Selhausen test site. It covers an area of 14 by 14 m and is situated in the middle of a gently sloping agricultural field. The soil type is a Haplic Luvisol with a silt loam texture and a relatively high stone fraction of about 12% in the top soil. In the Selhausen area a mean annual

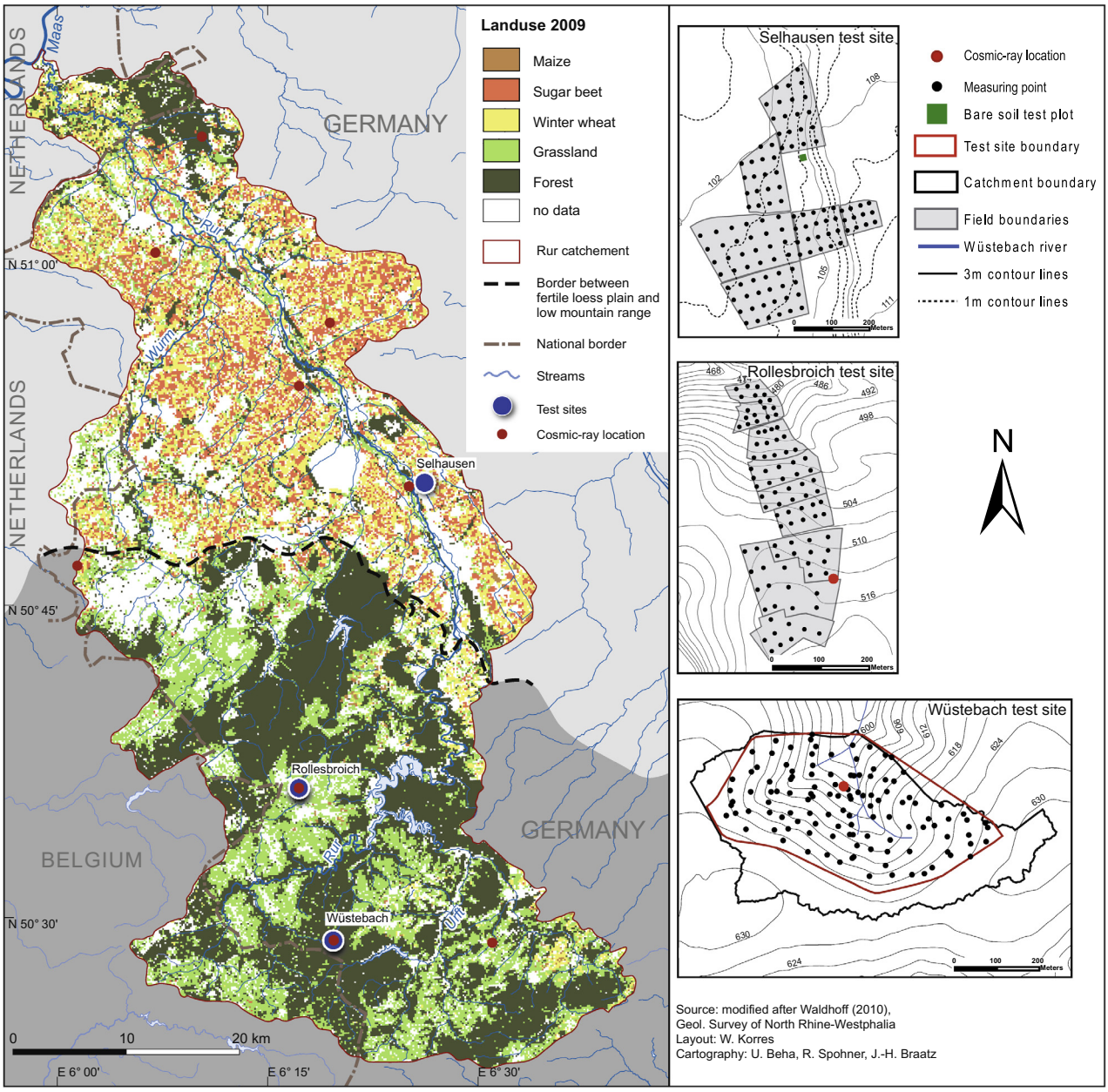

Fig. 1. The Rur catchment with the land use map of 2009, separated into the fertile loess plain in the north and the low mountain range in the south. The test sites Selhausen (arable land), Rollesbroich (grassland) and Wüstebach (forest) are depicted on the right side. Figure is modified after Cornelissen et al. (2014), Korres et al. (2010, 2013) and Waldhoff (2010).

precipitation of 690 mm was measured at the meteorological station at the Research Center Jülich, with slightly higher monthly values in June and July. In this dataset, the soil moisture was measured with a handheld ECH_2O probe (Decagon Devices, Pullman, WA). Following Oliver and Webster (1987) a nested approach, with a five stage nested design and random locations of the sampling points, was applied to determine topsoil moisture (<5 cm) between 26 April and 5 June 2007. This approach has the advantage of good coverage of sampling distances with a relatively small number of 48 sampling points. For further description of the dataset, see Herbst et al. (2009). This dataset is labeled MeasPlotBare (for MEASurement, PLOTscale, BARE soil) in the further analyses.

2.1.2. Field and sub-catchment scale

2.1.2.1. Selhausen fields. The intensively used arable land test site Selhausen covers an area of about 34.3 ha (Fig. 1), where crops (during our measurement period: sugar beet, wheat, rye, oilseed radish and fallow) are grown on gentle slopes (0° to 4°). The altitude ranges between 102 and 110 m a.s.l. Main soils types are (gleyic) Cambisol and (gleyic) Luvisol with a silt loam texture and a high amount of coarse material, originating from a former river terrace in the eastern part. Surface soil moisture was measured using a handheld FDR probe (Delta-T Devices Ltd., Cambridge, UK) between July 2007 and September 2008 on six different fields. For further description of the dataset see Korres et al. (2010). This dataset is labeled MeasFieldCrop (for MEASurement, FIELDscale, CROPs) in the further analyses.

2.1.2.2. Rollesbroich fields. The grassland test site near Rollesbroich (50°37′25″N, 6°18′16″E) covers an area of about 20 ha with nine fields of extensively used grassland (mainly perennial ryegrass and smooth meadow grass) with slopes from 0° to 10°, while

Table 1
Names, descriptions, scales (extent, spacing, support, compare Blöschl and Sivapalan, 1995) and labels of the different datasets. When a dataset consists of more than one soil layer, the layers are marked with L1, L2, and L3, respectively.

Data set	Landuse	Method	Mod./Meas.	Number of	Spacing		Extent		Support	Label
			Depth	Dates/Points	Spatial	Temporal	Spatial	Temporal	Spatial	
Selhausen plot	Bare soil	In-situ measurement	0–5 cm	10/48	0.5–2 m	1–7 days	14 m	6 weeks	6 cm	MeasPlotBare
Selhausen fields	Crops	In-situ measurement	0–6 cm	10/118	50 m	35 days	1.2 km	2 years	6 cm	MeasFieldCrop
Rollesbroich fields	Grassland	In-situ measurement	0–6 cm	8/96	50 m	35 days	1 km	2 years	6 cm	MeasFieldGrass
Wüstebach SoilNet L1	Forest	In-situ measurement	5 cm	730/112	5–50 m	1 day	800 m	2 years	6 cm	MeasSubForest L1
Wüstebach SoilNet L2	Forest	In-situ measurement	20 cm	730/112	5–50 m	1 day	800 m	2 years	6 cm	MeasSubForest L2
Wüstebach SoilNet L3	Forest	In-situ measurement	50 cm	730/112	5–50 m	1 day	800 m	2 years	6 cm	MeasSubForest L3
Wüstebach HydroGeoSphere L1	Forest	Modeling	5–15 cm	730/805	5–10 m	1 day	800 m	2 years	5–10 m	ModSubForest L1
Wüstebach HydroGeoSphere L2	Forest	Modeling	15–35 cm	730/805	5–10 m	1 day	800 m	2 years	5–10 m	ModSubForest L2
Wüstebach HydroGeoSphere L3	Forest	Modeling	35–75 cm	730/805	5–10 m	1 day	800 m	2 years	5–10 m	ModSubForest L3
Danubia L1	Crops/bare soil	Modeling	0–20 cm	361/20299	150 m	1 day	40 km	1 year	150 m	ModCatchCrop L1
Danubia L2	Crops/bare soil	Modeling	20–60 cm	361/20299	150 m	1 day	40 km	1 year	150 m	ModCatchCrop L2
ALOS	Crops/bare soil	Remote sensing	0–10 cm*	8/861138	15 m	46 days	40 km	2 years	15 m	RS15mCatchCrop
ENVISAT	Crops/bare soil	Remote sensing	0–3 cm*	10/18290	150 m	35 days	40 km	1 year	150 m	RS150mCatchCrop
Cosmic Ray	All	Measurement	0–12/70 cm**	330/9	1–20 km	1 day	70 km	2 years	600 m	CosmicCatchAll

* Approximately.
** Under wet/dry conditions.

altitude ranges from 474 to 518 m a.s.l. Average annual precipitation of 1033 mm was measured at a meteorological station 9 km west (altitude 505 m) of the test site. Similar to the other test sites, the precipitation does not show a pronounced seasonality. Dominant soils are (gleyic) Cambisol, Stagnosol and Cambisol–Stagnosol with a silt loam texture and a high amount of soil organic matter and high porosity in the topsoil, especially in the lower northern part. The measurement setup was the same as in the Selhausen fields dataset, but onnine different fields. Surface soil moisture was measured using a handheld FDR probe (Delta-T Devices Ltd., Cambridge, UK) between June 2007 and September 2008, for more details see Korres et al. (2010). This dataset is labeled MeasFieldGrass (for MEASurement, FIELDscale, GRASSland) in the following analyses.

2.1.2.3. Wüstebach SoilNet. The SoilNet dataset is a measured dataset at the Wüstebach test site, a small sub-catchment with an area of 27 ha (Fig. 1) within the river Rur catchment (Bogena et al., 2010). The dominant vegetation type is Norway spruce (90% coverage) on a relief with slopes up to 6°. The altitude ranges from 598 to 628 m a.s.l. and the mean annual precipitation is 1220 mm. On the hillslopes we found ground water distant soil types Cambisols and Planosol–Cambisols and ground water influenced soil types near the Wüstebach river (Planosols, Gleysols and Halfbogs) with a silty clay loam with a medium to very high fraction of coarse material (Richter, 2008). Soil moisture data was measured in three depths with a wireless sensor network (SoilNet) using ECH_2O probes (Decagon Devices, Pullman, WA). 74 measurement locations are arranged in a 60 by 60 m grid to get a sufficient spatial coverage (Rosenbaum et al., 2012). The remaining 76 locations are distributed randomly in order to sample the small scale variability. For our analysis only sensors without large data gaps in the 2 years of measurements (2010 and 2011) were chosen. We used instantaneous values measured at noon of every day. For further information about the sensor network SoilNet, see Bogena et al. (2010) and Rosenbaum et al. (2012). This dataset is labeled MeasSubForest (for MEASurement, SUB catchment scale, FOREST).

2.1.2.4. Wüstebach HydroGeoSphere. The fully coupled surface–subsurface flow model HydroGeoSphere (Goderniaux et al., 2009; Panday and Huyakorn, 2004) was applied to the Wüstebach subcatchment. The model was set up to include the influence of the bedrock and was calibrated using data from the SoilNet dataset from 2010, therefore the comparative analysis of these two datasets refers to the year 2011. The modeled soil layers correspond to the measurement depths in the SoilNet dataset (Cornelissen et al., 2014). For further model description, calibration, validation and parameterization information of the HydroGeoSphere model for this dataset, see Cornelissen et al. (2014). This dataset is labeled ModSubForest (for MODdeling, SUB catchment scale, FOREST).

2.1.3. Catchment scale

2.1.3.1. Danubia. The ecohydrological model components of the DANUBIA simulation system (Barth et al., 2004; Barthel et al., 2012) were used to generate daily soil moisture maps for cereals, sugar beet, maize and bare soil in the fertile loess plain. DANUBIA is a process based model describing the dynamic interaction of various environmental processes, including water fluxes affected by dynamic crop growth and agricultural management. For further information on the Danubia dataset and on parameterization and validation of the model for the river Rur catchment, see Korres et al. (2013). This dataset is labeled ModCatchCrop (for MODdeling, CATCHment scale, CROPs) below.

2.1.3.2. ALOS. The surface soil moisture of the ALOS dataset was retrieved using a dual-polarization L-band SAR (synthetic aperture

radar) retrieval algorithm for the three most common land cover types in the area of the fertile loess plain, i.e. bare soil, sugar beet, and winter wheat. For this algorithm coherent-on-receive dual polarimetry mode (FBD) data from the PALSAR radar instrument on the ALOS satellite platform was used. A biomass and surface roughness correction of the signal was achieved by applying a dual polarimetric H/alpha decomposition and using this increased amount of observables for the correction (Koyama and Schneider, 2014). The computation of the soil moisture was conducted for 8 ALOS overflight dates with an orbit repeat cycle of 46 days between May 2008 and September 2009. This dataset is labeled Rs15mCatchCrop (with Rs15m for Remote Sensing with 15 m spatial resolution, CATCHment scale, CROPs).

2.1.3.3. ENVISAT. For the ENVISAT dataset surface soil moisture was retrieved using single C-band SAR wide-swath (WS) single look complex (SLC) data from the ASAR instrument on the ENVISAT satellite platform. The semi-empirical retrieval algorithm from Rombach and Mauser (1997) modified by Loew et al. (2006) was used to correct for vegetation and surface roughness effects. Soil moisture for pixels of bare soil, cereals and root crops in the fertile loess plain were computed for 10 dates with an orbit repeat cycle of 35 days between February and October 2008. For more information about the ENVISAT dataset, see Koyama et al. (2010). This dataset is labeled Rs150mCatchCrop (with Rs150m for Remote Sensing with 150 m spatial resolution, CATCHment scale, CROPs) in further analyses.

2.1.3.4. Cosmic-ray. For this study, we also used soil moisture data from 9 cosmic-ray probes (type CRS1000, HydroInnova LLC, 2009) installed in the Rur catchment at a height of 1.5 m (Baatz et al., 2014). All land-use types (forest, crops, grassland, urban, in varying proportions) are represented by the locations of the cosmic-ray probes. Among all data sets, cosmic-ray probe measurements are the only measurements that cover both the northern and the southern part of the catchment (Fig. 1). The measurement principle is based on a strong inverse correlation of the measured fast neutron flux with the abundance of hydrogen atoms in the upper soil layer and thus can be used to determine soil water content (Zreda et al., 2008). The horizontal footprint of this measurement has an approximate radius of about 300 m around the cosmic-ray probe at sea level or somewhat less depending on air density (Desilets and Zreda, 2013). The sensors were calibrated to obtain daily averaged soil moisture values from May 2012 to July 2013 using the semi-empirical method of Desilets et al. (2010). Data gaps are due to malfunction of one or more probes at single dates. For more information about the locations of the probes and the dataset, see Baatz et al. (2014) and Bogena et al. (2013). This dataset is labeled CosmicCatchAll (with COSMIC for cosmic-ray probes, CATCHment scale, ALL indicating that all land use types are included).

2.2. Statistical analysis

2.2.1. Descriptive statistics

First the datasets were investigated using univariate descriptive analysis. For each dataset (and soil layer) the spatial mean soil moisture and soil moisture variability (expressed by the standard deviation (SD) and the coefficient of variation (CV)) were calculated. We computed regression equations between the CV and mean soil moisture using ordinary least squares. The coefficient of determination R^2 was used as a goodness-of-fit measure. Significance was tested using a p-value of 0.05. All analyses were conducted with R (R Core Team, 2014).

2.2.2. Geostatistics

The spatial autocorrelation structure was analyzed using a geostatistical analysis. The omnidirectional experimental semivariances γ of the measured variable Z were calculated as follows:

$$\gamma(h) = \frac{1}{2n(h)} \sum_{i=1}^{n(h)} [Z_i - Z_{i+h}]^2 \quad (1)$$

where $n(h)$ is the number of distant pairs within a given distance class, Z_i is the measured variable at location i and Z_{i+h} is the variable at locations separated from i by the distances h that fall within the distance class. The semivariances were calculated using the R library geoR (Diggle and Ribeiro, 2007). For the datasets with an extent below 1.2 km (see Table 1) we used a fixed number of eight equidistant distance classes. For the datasets with an extent above 1.2 km, smaller variogram classes were calculated for short distances (<3 km), to better represent those distances, where the largest changes can be expected.

An exponential variogram was fitted to the experimental semivariances, since this type generally provided the best fits:

$$\gamma(h) = c_0 + c_1 \left[1 - \exp\left(-\frac{h}{r}\right)\right] \quad (2)$$

where h is the distance class separation distance, c_o is the nugget semivariance, c_1 is the structural semivariance and r is the distance parameter defining the spatial extent of the model. The total sill ($c_o + c_1$) defines the semivariance at which the variogram flattens out and is furthermore simply termed as sill. The effective range (a; the distance at which γ equals 95% of the sill) is approximately three times the parameter r. The range value characterizes the maximum distance of autocorrelation. To minimize the effect of nonstationarity for the fitting of the variogram model we reduced the maximum range for the model fitting to 300 m for the datasets MeasSubForest and ModSubForest, to 3 km for the datasets Rs15mCatchCrop and Rs150mCatchCrop and to 15 km for the ModCatchCrop dataset. It is important to note that the results are apparent semivariances and autocorrelation lengths, which may be biased by the difference of scale of natural variability and measurement scale in terms of spacing extent and support (Western and Blöschl, 1999). The apparent autocorrelation lengths always increase with increasing spacing, extent or support and the apparent variance increases with increasing extent, decreases with increasing support, and does not change with spacing (Western and Blöschl, 1999). The analysis of the spatial autocorrelation is limited to the datasets that are non-sparse in the temporal or spatial domain. This restriction was made to be able to compute either stable geostatistical parameters (semivariances, variogram model parameters) for the spatial patterns or to analyze the development of the spatial autocorrelation over time. The validity of the computed geostatistical parameters from a sparse dataset in the spatial domain may then be assessed through the temporal stability of the parameters. The Cosmic Ray dataset fulfilled the prerequisite to be non-sparse on the temporal domain, but since only 9 measuring points are available, geostatistical parameters cannot be computed and therefore this dataset was also discarded from the autocorrelation analysis. Consequently, only the datasets MeasSubForest, ModSubForest, ModCatchCrop, Rs15mCatchCrop and Rs150mCatchCrop were used for the geostatistical and the following fractal analysis.

2.2.3. Fractals

In addition, fractal geometry (Mandelbrot, 1977) was used to describe self-similar patterns of variation using simple parameters (e.g. fractal dimension). Mandelbrot (1977) introduced the term fractal to describe any function for which the Hausdorf-Besicovich dimension (D) exceeds the topological dimension (e.g., 1 for lines or 2 for areas). For such functions, the Hausdorf-Besicovich

dimension is commonly termed fractal dimension (Goodchild and Mark, 1987). The values for the fractal dimensions (D) for spatial data varies between 2 (topological dimension for areas) and 3. They provide information about the spatial structure of a dataset. For example, rough surfaces with a low autocorrelation structure have high fractal dimensions (D close to 3) and smooth surfaces with similar values in adjacent areas and a high autocorrelation structure have low fractal dimensions (D close to 2). The other important concept in the context of fractals is self-similarity. In a statistical sense, the concept of self-similarity means that a portion of an entity looks similar to the whole entity if enlarged or reduced to the appropriate scale (Gao and Xia, 1996). This means, that a single fractal dimension applies to all scales of a surface. However, Sun et al. (2006) stated that in geosciences various natural processes operate at different scales, leading to varying fractal dimensions, that are only constant over certain ranges of scales, separated by distinct scale breaks (Burrough, 1983; Klinkenberg and Goodchild, 1992; Mark and Aronson, 1984). This concept is called multi-fractal and can be used to describe nested scales of variability.

The fractal dimension (D) can be estimated from the slope of a double logarithmic (log–log) plot of an experimental semivariogram (Burrough, 1983; Mark and Aronson, 1984):

$$D = 3 - B/2 \quad (3)$$

where B is the slope of the regression line. In case of multi-fractal behavior the regression lines were calculated for the different segments of the double logarithmic plot. With the segmented regression method by Muggeo (2003; R library segmented) the regression lines are fitted and breakpoints are computed, which provide an objective method to determine the fractal dimension (D) from the slope of the different regression lines and associated scale breaks (SB). A maximum of two breakpoints was computed.

3. Results and discussion

The spatial and temporal scales of the different datasets are very versatile. We analyzed soil moisture datasets with a spatial extent ranging from 14 m (bare soil plot) up to the whole Rur watershed (Cosmic Ray sensors at 9 different locations) with a temporal extent of one or two years. An exception is the bare soil plot dataset with only 6 weeks (10 dates), which therefore is prone to biases in the soil moisture conditions. In case of the MeasPlotBare data set, we measured low surface soil moisture values at the first six dates, leading to a very low overall mean soil moisture of 15.2 vol.% for the whole dataset (Table 2). In addition, spacing of the datasets is very different for the various datasets, with values smaller than 1 m up to several kilometers in the spatial domain and daily measurements (here sometimes even aggregated to daily measurements from the original datasets) to measurement intervals of about 40 days in the temporal domain, e.g. due to the orbit repeat cycle of the satellite overpasses.

The highest mean soil moisture values can be found in datasets measured at or modeled for elevated areas in the southern hilly part of the Rur catchment with higher amounts of precipitation (e.g., MeasFieldGrass, MeasSubForest, and ModSubForest). The mean value in these datasets declines with deeper soil layers. This is caused by the lower porosity in the deeper soil layers. Lower mean soil moisture values can be found in the datasets for the northern part of the catchment (e.g., MeasFieldCrop, Rs15mCatchCrop, Rs150mCatchCrop, ModCatchCrop). Consistently, the strong gradient in mean soil moisture from north to south is visible in the site specific mean soil moisture measured at the catchment wide CosmicCatchAll dataset, as indicated by Baatz et al. (2014). The variation of the mean soil moisture values between the datasets from the northern part of the catchment are caused by the different soil moisture states at different years of data acquisition and the sparse and predefined dates of the satellite overpasses.

Table 2
Descriptive statistics of the different datasets. Mean values are calculated as the mean value of all spatial mean values (spatiotemporal mean) within one dataset, standard deviation (SD) and coefficient of variation (CV) values are calculated as the mean value of all spatial SD and CV values, respectively.

Label	Soil moisture (mean values)		
	Mean (vol.%)	SD (vol.%)	CV
MeasPlotBare	15.24	2.77	0.20
MeasFieldCrop	26.15	3.90	0.16
MeasFieldGrass	43.08	4.35	0.10
MeasSubForest L1	41.61	12.55	0.32
MeasSubForest L2	39.56	9.48	0.24
MeasSubForest L3	33.81	9.37	0.28
ModSubForest L1	41.61	8.69	0.22
ModSubForest L2	37.86	7.12	0.20
ModSubForest L3	33.49	5.19	0.16
ModCatchCrop L1	27.66	4.01	0.15
ModCatchCrop L2	25.59	4.53	0.18
Rs15mCatchCrop	24.05	2.11	0.10
Rs150mCatchCrop	31.35	2.68	0.09
CosmicCatchAll	32.72	8.19	0.26

The highest variability of soil moisture (expressed by the coefficient of variation, CV) can be found in the measured data from the forest sub catchment (Table 2). This variability with a CV up to 0.32 is much higher compared to CVs of the arable land and grassland test sites with values of the CV less than 0.18. This difference in variability is caused by the influence of the stronger topography within the forest catchment with drier upslope areas and constantly wetter downslope areas influenced by a shallow ground water table and by the heterogeneity within the forest stand with lower moisture values around the trees and higher values in the interspaces between tree stands. Comparable values for forest test sites (Grant et al., 2004) and grassland test sites (Western et al., 1999b) can be found in the literature (Zucco et al., 2014). The small CV values for the remotely sensed surface soil moisture values can be explained by the larger spatial support of the sensors, measuring a larger area and therefore averaging the small scale variability over a larger area, compared to the point measurements at the ground level. It should be mentioned explicitly that the remotely sensed surface soil moisture values are only available for arable and grassland sites, but not for forests, since the radar signal does not penetrate the dense vegetation cover of forest areas. For the MeasPlotBare dataset the high CV value of 0.2 is caused by the very low mean soil moisture values. High soil moisture variability is also found for the CosmicCatchAll dataset (CV = 0.26). This can be explained by (i) the fact, that these measurements cover both the drier northern and the wetter southern part of the Rur catchment, (ii) the small number of measurement sites and (iii) the coverage of all land use types in varying proportions.

The temporal dynamics of the datasets show a direct impact of precipitation events on the soil water content which results in an inverse relationship of mean soil moisture and coefficient of variation (Fig. 2). With increasing soil moisture, the CV typically decreases. Except for the period from May to June 2011, a slight increase in the standard deviation with drying soil moisture conditions in the MeasSubForest dataset can also be seen. The datasets from the forest catchment (MeasSubForest and ModSubForest) have a much larger temporal variability which exceeds 25 vol.% as compared to the ModCatchCrop dataset with about 15 vol.% (Fig. 2). This is a result of a much larger maximum porosity of the soils in the forest catchment, causing higher maximum soil water contents during the winter period. Furthermore, the strong influence of the soil parameterization (porosity) can be noted, leading to a distinct upper limit (about 34 vol.% for ModCatchCrop

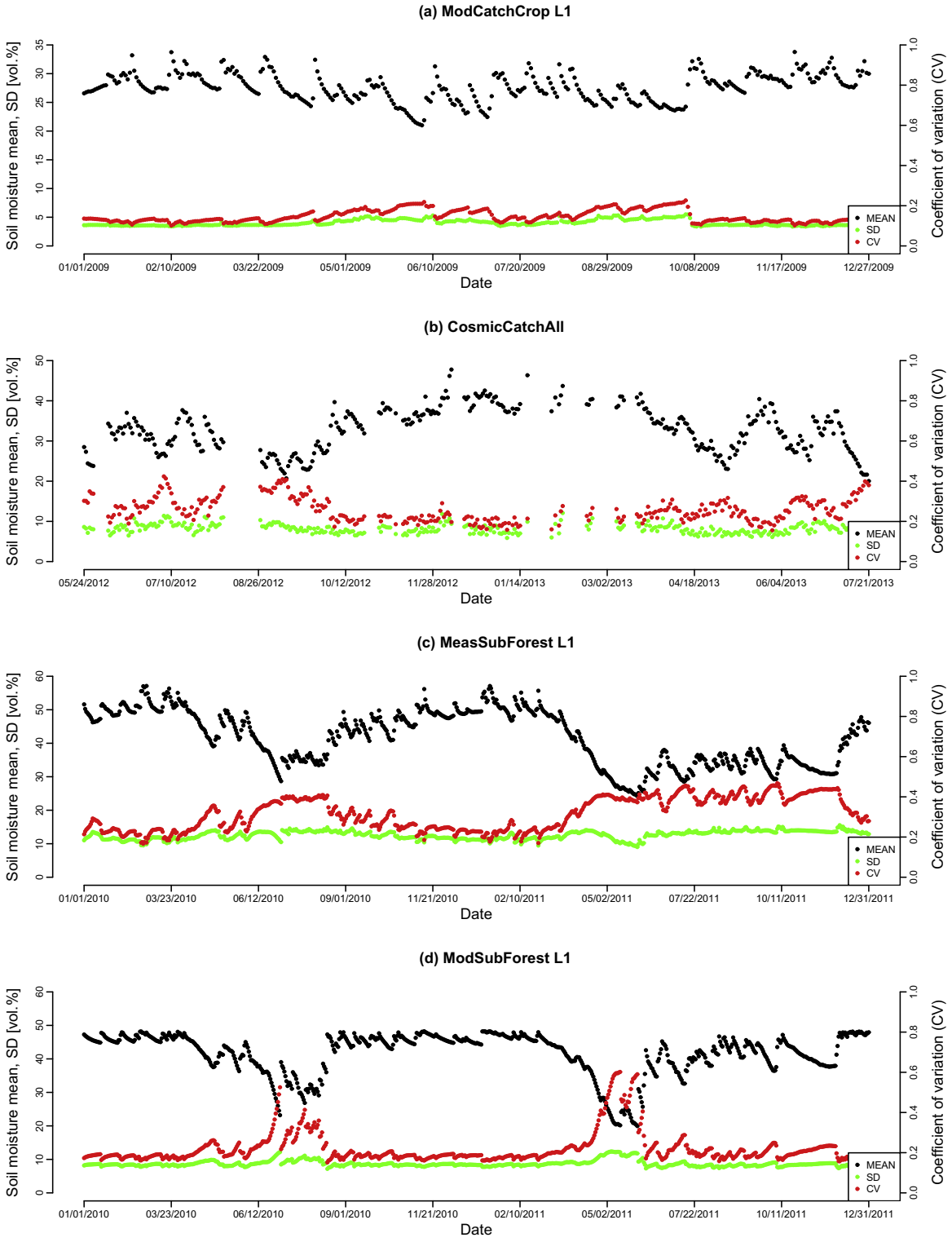

Fig. 2. Time series of daily mean soil moisture, daily standard deviation (SD) and the coefficient of variation (CV) of four exemplary datasets. The data gaps in the CosmicCatchAll time series are due to malfunction of at least one of the measuring devices at that day. The model used to derive the ModSubForest dataset was calibrated with the data from 2010 of the MeasSubForest dataset.

and 48 vol.% for ModSubForest) in the modeled soil moisture time series (Fig. 2).

3.1. Link between soil moisture mean and variability

In our study, we found a negative correlation between mean soil moisture and soil moisture variability expressed by the coefficient of variation (CV) in all datasets (Fig. 3). The slopes of the linear regression between mean soil moisture and the CV varies between −0.015 for the ModCatchCrop L2 dataset and −0.006 for the MeasSubForest L3 and the Rs15mCatchCrop dataset. The linear regression for MeasFieldCrop and the MeasFieldGrass dataset are not significant at the $p = 0.05$ level and are therefore discarded in further analyses. Some authors (Choi and Jacobs, 2007; Hu et al., 2008) use an exponential fit

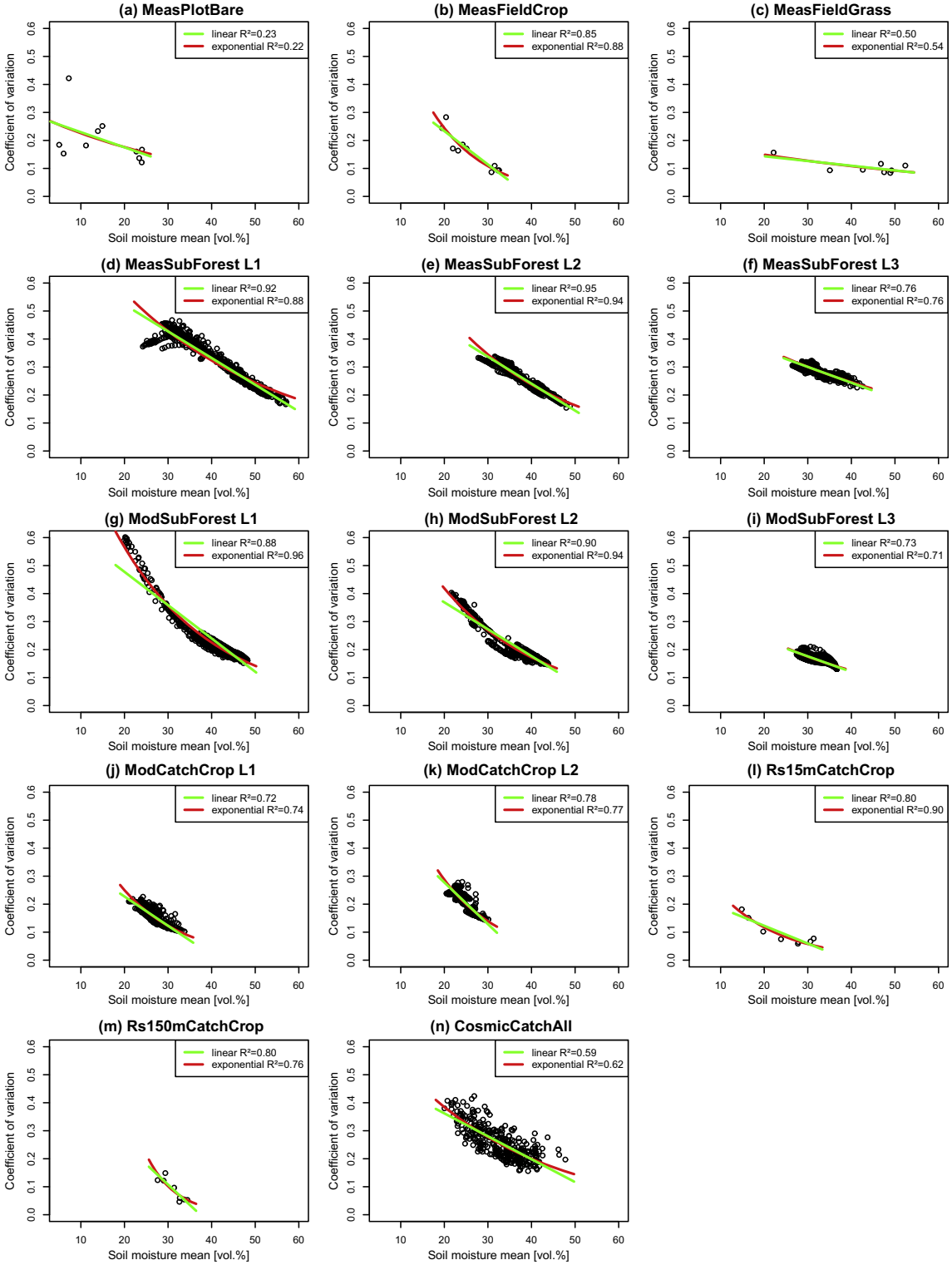

Fig. 3. Scatterplots of the soil moisture mean and the coefficient of variation for all analyzed datasets and soil layers. A linear and an exponential regression with the associated R^2-values are plotted in green and red. Regressions are significant on the $p = 0.05$ level with the exceptions of (a) MeasPlotBare and (c) MeasFieldGrass.

to describe this relationship, because at drier soil moisture states the relationship deviates strongly from a linear relationship. In our analysis, the exponential fit results in a significant increase of the R^2 value in only a few cases, therefore we used the linear relationships in our analysis for better comparability.

For the datasets measured in and modeled for the flat agricultural area in the northern part of the catchment (MeasFieldCrop, ModCatchCrop, Rs15mCatchCrop, Rs150mCatchCrop) we found no evidence for the influence of lateral water fluxes on the soil moisture patterns and relatively homogeneous soil properties over large areas (Korres et al., 2013). Since soil moisture is limited by the wilting point during very dry periods and by the porosity in case of saturated conditions, decreasing soil moisture variability with increasing mean soil moisture is to be expected in datasets

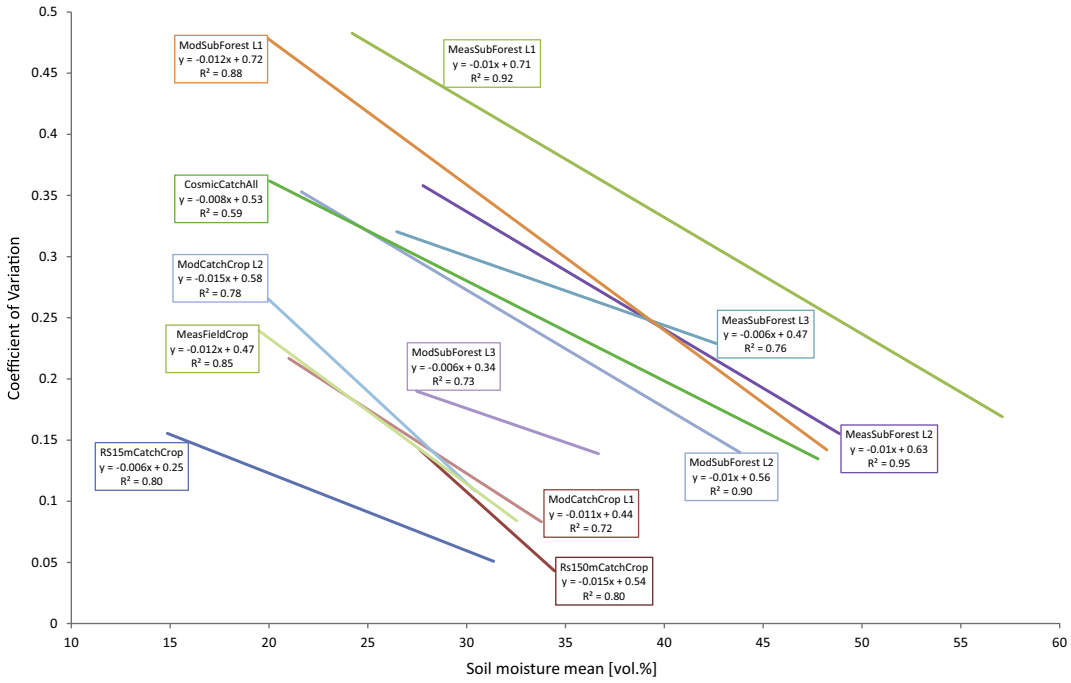

Fig. 4. Lines of the linear regression of the soil moisture mean and the coefficient of variation. Name of the dataset, the regression equation and the associated R^2-value are depicted in the boxes with the same color as the regression line. Only significant regressions on the $p = 0.05$ level are shown.

with homogeneous soil properties. During the vegetation period we found higher evapotranspiration rates and high spatial variability of transpiration for the different crops (mainly cereals, sugar beet, and maize) in the ModCatchCrop dataset. This is caused by (i) differences in the growth periods of the different crops, (ii) by the varying evapotranspiration of the different plants and (iii) management effects (e.g., planting, harvesting, and fertilization). This results in a large inter-field variability at the dry soil moisture state in intensively used agricultural areas. The influence of transpiration is spatially more homogeneous in the forest and the grassland test sites (MeasFieldGrass, MeasSubForest, ModSubForest). However, generally higher soil moisture values and the influence of a stronger topography result in lateral flow processes. At the forest test site, we found higher spatial soil moisture variability at the dry state compared to the wet state. This is due to the slower drying rates of the increasingly fine-textured soils in the valley area with convergent lateral flow and due to groundwater influence (Rosenbaum et al., 2012). Generally, upslope areas showed significantly lower mean soil moistures and a larger range of soil moisture than the groundwater-influenced areas in the valley (Rosenbaum et al., 2012).

The relationship between mean soil moisture and coefficient of variation of the different datasets are shown in Fig. 4. For a better comparability of the slopes only the linear relationships are illustrated, even though we found a slightly better fit of an exponential function for the datasets MeasSubForest L1, MeasSubForest L2, ModSubForest L1, ModSubForest L2, and Rs15mCatchCrop. The datasets cover quite different soil moisture ranges. For example, the radar remote sensing dataset from Rs15mCatchCrop covers dry soil moistures ranging from 15 vol.% to 31 vol.%, whereas the MeasSubForest dataset taken in the top layer of the forest subcatchment shows high mean soil moisture values ranging from 25 vol.% up to 56 vol.%. The CV values at an average soil moisture of 30 vol.% varies from about 0.06 for the Rs15mCatchCrop dataset to 0.44 for the uppermost layer of the measured forest data set (MeasSubForest). For agriculturally used areas the CV values at 30 vol.% for the different data sets (ModCatchCrop L1, ModCatchCrop L2, Rs150mCatchCrop and MeasFieldCrop) converge at about 0.14, while the forested test sites show significantly larger CV values. In general, the CVs of the modeled dataset ModSubForest are lower than the measured CVs from the MeasSubForest dataset for their associated soil layer. In both of these datasets the CV value decreases with deeper soil layers. This is due to the decreasing porosity with soil depth (Rosenbaum et al., 2012). In contrast to the decreasing CV with soil depth in the forest sub catchment, the variability in the top layer of the ModCatchCrop dataset is equal to or even slightly lower as compared to the lower soil layer. This can result from a homogenization of the top soil caused by agricultural management (e.g., ploughing and harrowing) and from the shift in periods of high plant water uptake from the root zone of the different crops. The development of winter wheat is completed by the end of June or beginning of July, whereas sugar beet and maize start their growing cycle later in the year and finish their development with their harvest in September, October or November (Korres et al., 2013). While the upper soil layers receive water from precipitation, which has a homogenizing effect on the soil moisture patterns, percolation to deeper soil layers is greatly reduced or stopped during the second half of the vegetation period. Thus, the homogenizing effect of water recharge is missing in deeper soil layers during that time. The CosmicCatchAll dataset provides a special case, because it contains point measurements from locations with very different soil and land use conditions on grassland, arable land and forest or mixed proportions of these different land use classes. This data set shows an intermediate CV value between 0.15 and 0.37 (Fig. 4).

Moreover, our results show that spatial variability of soil moisture not only depends on mean soil moisture, but also varies with spatial scale (spatial extent and spatial support) of the analysis. This behavior was also found by Famiglietti et al. (2008), Manfreda et al. (2007) and Rodriguez-Iturbe et al. (1995). Previously conducted individual analyses of the different datasets showed a decrease of spatial variability with (i) decreasing spatial

extent (in Koyama et al., 2010) and (ii) increasing spatial support (in Bogena et al., 2010; Korres et al., 2013). However, such a relationship between our different datasets cannot be found (Fig. 4), because the effect of different spatial extent and support between the datasets is often masked and superimposed by the larger actual variability of the natural processes within the single datasets. Hence, the observed variability between the datasets (Fig. 4) is more influenced by the natural processes than the measurement or modeling scale.

To avoid interdependencies between the two statistical moments mean and variability we used mainly the CV as a measure for variability in our analyses. Regarding the relationship between the standard deviation and mean soil moisture, only the MeasSubForest L1 and L2 datasets show a convex shape with the maximum spatial variability in the intermediate soil moisture state at about 40 vol.%. (Rosenbaum et al., 2012). This follows the theoretical unimodal shape of the relationship between standard deviation and mean soil moisture (Vereecken et al., 2007). At wet conditions, the variability is mainly controlled by hydraulic conductivity and porosity. During the drying process, the spatial differences of soil properties lead to an increase of variability at intermediate moisture conditions. Further drying by evapotranspiration then again leads to a decrease of variability at dry soil moisture conditions (Famiglietti et al., 1998; Pan and Peters-Lidard, 2008; Vereecken et al., 2007). Other datasets showed a positive linear relationship (MeasPlotBare, MeasFieldGrass, MeasSubForest), a negative linear relationship (MeasFieldCrop, ModSubForest L1, ModSubForest L2, ModCatchCrop L1, ModCatchCrop L2, Rs150mCatchCrop) or no significant linear relationship on a $p = 0.05$ level (ModSubForest L3, CosmicCatchAll, Rs15mCatchCrop). These linear relationships can be interpreted as the drying or the wetting arm of the convex relationship between standard deviation and mean soil moisture representing dry to intermediate soil moisture conditions (positive linear relationship) or intermediate to wet soil moisture conditions (negative linear relationship). Only the MeasFieldGrass dataset due to very heterogeneous soil properties (Korres et al., 2010) and the ModSubForest L1 and L2 datasets, because of not fully simulating the drying arm of the unimodal relationship (Cornelissen et al., 2014) did not fit in this interpretation.

3.2. Geostatistical analysis

Experimental semivariances and fitted exponential variograms from an early date in the year (representing typical wet conditions) and from a date at the end of the main vegetation period (representing typical dry conditions) were selected to illustrate the influence of the vegetation on soil moisture autocorrelation (Fig. 5). As expected from the standard deviations from Table 2, the datasets from the forest catchment MeasSubForest and ModSubForest show the largest sill values with a decreasing sill with decreasing soil depth. The ModCatchCrop dataset shows generally lower sill values. The lowest mean sill values were computed from datasets from radar remote sensing. The explanation of the differences in the sill values follows the previous discussion on the spatiotemporal SD and CV values.

The range parameter can be used to describe the break between spatially correlated and uncorrelated values. Hence it provides information about the spatial organization of soil moisture patterns. Changes of the range values with time can be assigned to the varying impact of different processes within a dataset. Differences in the magnitude of the range values can be assigned to different dominating processes, parameters or structures. We found mean variogram ranges for the MeasSubForest dataset of 122, 149 and 254 m for the Layers L1, L2 and L3, respectively. The mean variogram ranges from ModSubForest (110, 142, 175 m for depths L1, L2 and L3, respectively) have a similar increasing trend with increasing soil depths. This is in agreement with the MeasSubForest dataset. In the ModSubForest dataset the ranges significantly increase in all soil layers with decreasing mean soil moisture, meaning we computed larger range values at drier soil moisture conditions. The larger range values can be explained by a more pronounced spatial organization at drier conditions, which is caused by effects of elevation with drier upslope areas and constantly wetter downslope areas influenced by a shallow ground water table. Under wet conditions, the smaller range is mainly influenced by the small scale variability in porosity (Cornelissen et al., 2014). For the ModCatchCrop dataset we found much larger mean range values (14 km and 11 km, for L1 and L2, respectively) which show a close similarity to the semivariance of the soil parameters calculated from the soil map. Thus, the larger range values (>10 km) are mainly linked to the pattern of the different soil types (Korres et al., 2013). In the radar remote sensing datasets (Rs15mCatchCrop and Rs150mCatchCrop) for the same region, we cannot identify the influence of large scale differences in soil parameters in the variograms (Fig. 5). We found mean range values of 432 m for the Rs15mCatchCrop and 711 m for the Rs150mCatchCrop dataset. These smaller range values are associated with the land use structure (field size) of that area. The large variability at a small spatial scale is caused by different agricultural crops on neighboring fields leading to spatially variable evapotranspiration rates, hence to variable water uptake and soil moisture values. Conversely, this small scale variability cannot be identified in the range values of the modeled ModCatchCrop dataset. This indicates that the method of the surface roughness and biomass correction of the Rs150mCatchCrop dataset emphasizes the influence of different crops on the soil moisture patterns stronger than the model. The influence of the large scale patterns of different soil types can only be found in the modeled ModCatchCrop dataset but not in the remote sensing dataset. This underlines the importance of proper soil parameterization as input data for environmental models and for proper modeling of soil moisture patterns.

A graphical synopsis of the geostatistical analysis concerning the range and the sill can be seen in Fig. 6. Sill and range values of all days of the different datasets are plotted and despite the scattering of the daily data, three bigger clusters can be identified: (i) modeled and measured datasets from the forest sub-catchment with large sill values and small range values, (ii) remotely sensed datasets from the northern part of the Rur catchment with small to medium sill values and medium range values, and (iii) modeled dataset from the northern part of the Rur catchment with medium sill values and large range values.

As the analyses of the temporal evolution of the experimental semivariances of the different datasets is of great interest, we used the daily calculated experimental semivariances for the different distances of each dataset and plotted contour plots with the distances on the x-axis, the day of the analyzed year (DOY) on the y-axis and the color-coded semivariances (Fig. 7).

The pattern of the ModSubForest dataset (Fig. 7d and e) showed a period around DOY 140 with high semivariances, caused by a period of low precipitation and low mean soil moisture values (Cornelissen et al., 2014). This can again be explained by elevation effects as described in the previous section. For the ModSubForest dataset we computed significant negative correlations between mean soil moisture and the sill with a large proportion of the explained variance of these datasets ($R^2 = 0.79$ for L1 and $R^2 = 0.78$ for L2). This shows the large influence of meteorological forcing in combination with the spatial distribution of soil parameters on the simulated soil moisture patterns.

The temporal behavior of the semivariance pattern of the measurements of the MeasSubForest dataset (Fig. 7a and b) shows large differences compared to the pattern of the modeled values from ModSubForest (Fig. 7d and e). The MeasSubForest dataset

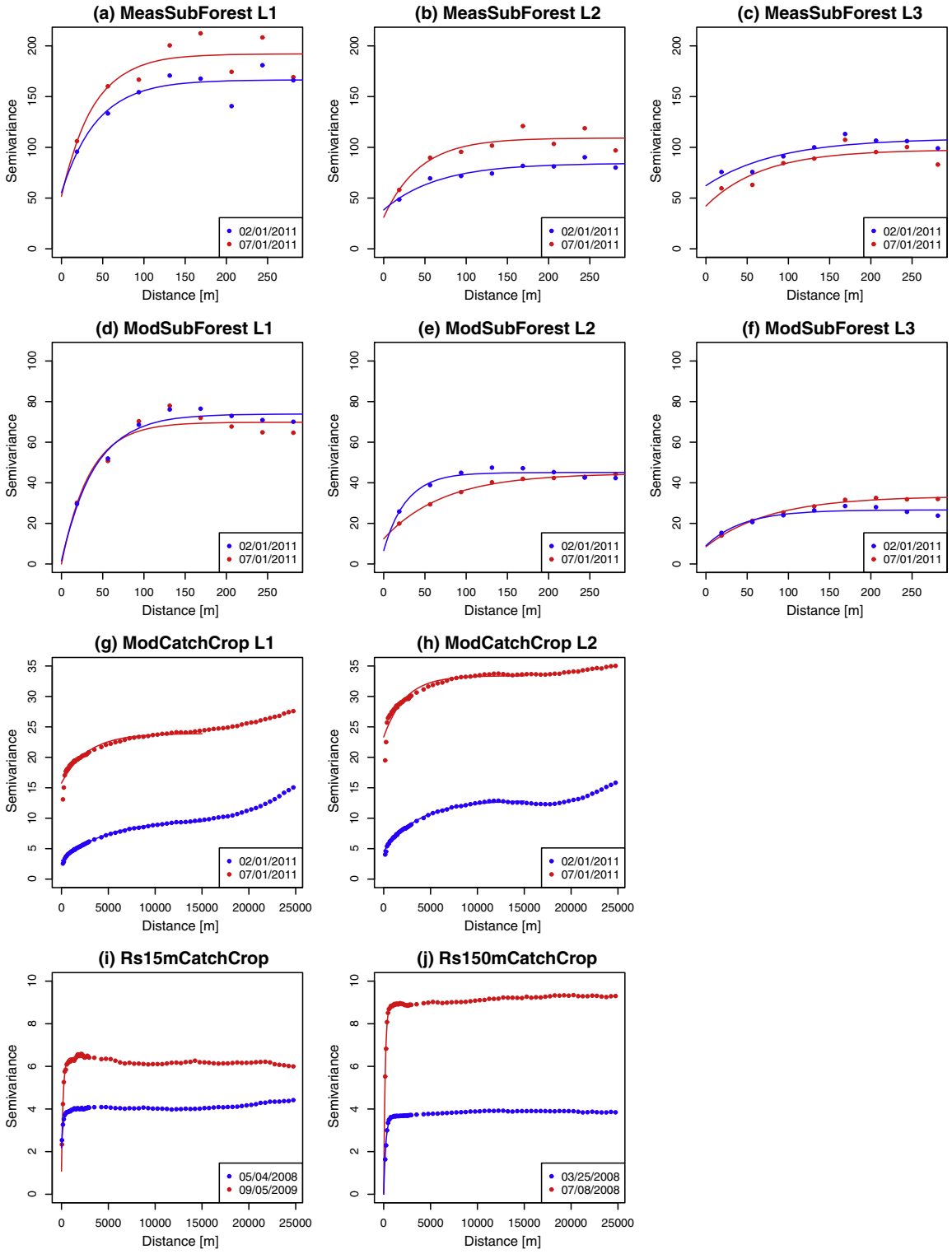

Fig. 5. Experimental semivariances and fitted exponential semivariogram models of the different soil moisture datasets for a typical dry (red) and wet (blue) situation, respectively. The geostatistical analysis is limited to the datasets that are non-sparse in the temporal or spatial domain. Thus, the datasets MeasPlotBare, MeasFieldCrop, MeasFieldGrass and CosmicCatchAll were discarded from the analysis.

shows the highest semivariance values in all soil layers in the second half of the year 2011. The reason for the different behavior between these two datasets in the second half of 2011 can be attributed to the differences of the mean soil moisture (see Fig. 2c and d). After very dry soil moisture conditions in June, the ModSubForest dataset reaches very high soil moisture values near the maximum porosity after precipitation events between July and the end of the year. However, the mean soil moisture values for the MeasSubForest datasets during that time never reached the maximum porosity, as for example in February 2011 (Fig. 2). The same

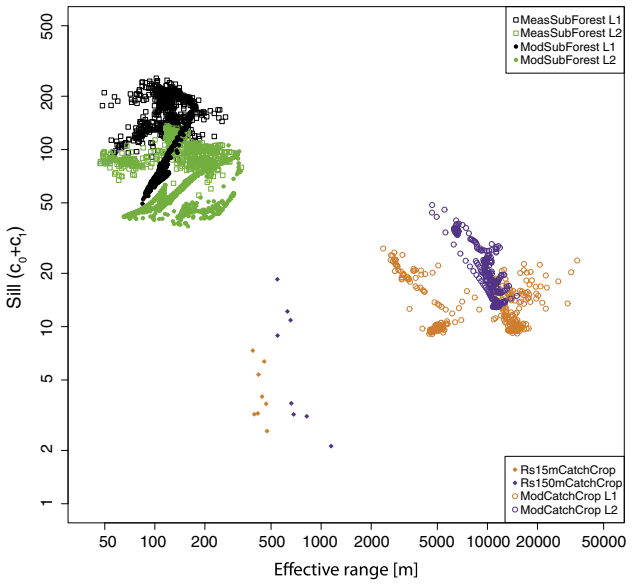

Fig. 6. Log–log plot of the relationship of the sill values of the fitted variogram models and the associated effective range. The geostatistical analysis is limited to the datasets that are non-sparse in the temporal or spatial domain. Thus, the datasets MeasPlotBare, MeasFieldCrop, MeasFieldGrass and CosmicCatchAll were discarded from the analysis. On the *y*-axis $c_0 + c_1$ indicates that the nugget variance is included in the total sill.

differences are found in the second soil layer (not shown). The replenishment of soil water content by precipitation to values up to the maximum porosity in the ModSubForest dataset leads to a full reset of the soil moisture pattern with smaller sill values, whereas the soil moisture patterns of the MeasSubForest dataset with a high spatial variability were only marginally influenced by precipitation, replenishing only parts of the soil pores and keeping the overall soil moisture pattern intact. Reasons for that difference might be errors in the precipitation input into the model, due to errors in the measurement or the applied correction algorithm or the simple modeling of the vegetation in ModSubForest. The heterogeneity of transpiration in the model only depends on soil moisture conditions, since the vegetation parameterization is spatially constant (Cornelissen et al., 2014). This example demonstrates the importance of (i) the correct model input (e.g., precipitation from measurements, soil parameters) and (ii) correct modeling of green water fluxes and runoff for the realistic modeling soil moisture patterns.

In the ModCatchCrop dataset (Fig. 7g and h) we notice two periods with higher semivariances, one around DOY 150 and another one around DOY 260. These two periods of higher variability are caused by the high heterogeneity of transpiration of the different plants on neighboring fields. The first peak is determined by the early biomass production and therefore high transpiration of winter cereals in contrast to later biomass production of sugar beet and maize. The second peak is determined by the discontinued transpiration caused by harvesting the winter cereals, contrasted by the high biomass production of sugar beet and maize. Between these two peaks there is a period of homogeneous transpiration rates with a diminished transpiration of the drying winter cereals and increasing transpiration of the growing sugar beet and maize plants. In this dataset significant negative correlations between mean soil moisture and the sill were determined, but with a far lower proportion of the explained variance ($R^2 = 0.36$ for L1 and $R^2 = 0.33$ for L2), indicating the strong influence of the vegetation on the soil moisture patterns and less influence of the meteorological forcing. Additionally, by comparing the semivariances between the ModSubForest and the ModCatchCrop dataset at very high soil moisture conditions near maximum capacity at the beginning and at the end of the year, the influence of the soil parameterization of the models on soil moisture patterns can be assessed. Here we found much larger variability of soil parameters (e.g., porosity, field capacity) in the forest sub-catchment resulting in higher semivariances, as compared to the more homogeneous loess plain.

3.3. Detection of scale breaks in the autocorrelation structure using fractals

For the fractal analysis we computed fractal dimensions (D) of the datasets ModCatchCrop L1, Rs15mCatchCrop and Rs150mCatchCrop for the same two days given in Fig. 4. We found multifractal behavior in all these datasets, showing at least one distinct scale break of the spatial variability over the analyzed range of scales (Fig. 8).

For the date 2/1/2009 of the ModCatchCrop dataset (Fig. 8a) we found a scale break around 17.5 km, with a high D value of 2.86 before the break and a medium D value of 2.5 after the break. At the beginning of the year the influence of the crops is negligible, so we can notice the influence of larger spatial variability and lower autocorrelation within soil types before the scale break and the influence of a larger spatial organization with a higher autocorrelation between soil types resulting in lower D values for distances after the scale break (for detailed soil information see Korres et al. (2013)). On 10/1/2009 (Fig. 8b), in addition to the scale break described above (SB2 in Fig. 8b), we found a second scale break (SB1) at a much smaller distance of about 400 m. This is associated with the specific field sizes in the northern part of the Rur catchment and again the influence of the vegetation (strongly varying evapotranspiration rates on neighboring fields). We computed the fractal dimensions and scale breaks for every day of every dataset. The scale break at larger distances (SB1 in Fig. 8a and SB2 in Fig. 8b) is stable throughout the whole year in the ModCatchCrop dataset. The scale break around 400 m was only observed at times, when the evapotranspiration rates on neighboring fields differ largely. Very similar scale breaks were found for the deeper soil layer L2 for the ModCatchCrop dataset (not shown). In the Rs150mCatchCrop dataset (Fig. 8e and f) we found only a scale break associated with the field sizes. At larger distances a slight change in the values occurs that might be caused by different soil types. However, these differences are too small to be significant and to be captured accurately with our analysis method. Unfortunately, the soil type scale break cannot be investigated further with the Rs150mCatchCrop dataset, because we have no data for the winter months with no vegetation influence and soil water content near saturation. In the Rs15mCatchCrop dataset (Fig. 8c and d) we also computed the scale break at field size, but at a slightly shorter distance of 258 and 276 m. The differences in the distances of the scale break associated to one process or parameter can be explained by the varying spatial scale (support) between the datasets for the scale break between 250 and 600 m. A source of error of our method is caused by the fitting procedure of the regression lines on the logarithmic scale, because small changes in the fitting lead to large differences in the scale break at larger distances. The most interesting result of the fractal analysis is the scale break B2 for the Rs15mCatchCrop dataset in Fig. 8c confirming the scale break found by the analysis on the modeled data from ModCatchCrop. While the scale break in the ModCatchCrop dataset might be caused by the soil parameterization using the available soil map as input, the soil moisture maps from Rs15mCatchCrop are processed independently from such input data. Hence, the results of the different datasets for the northern part of the Rur catchment complement and support each other.

For the MeasPlotBare dataset we were not able to compute a good and stable fit in the regression analysis, suggesting that a fractal or multifractal model is not appropriate for this dataset at

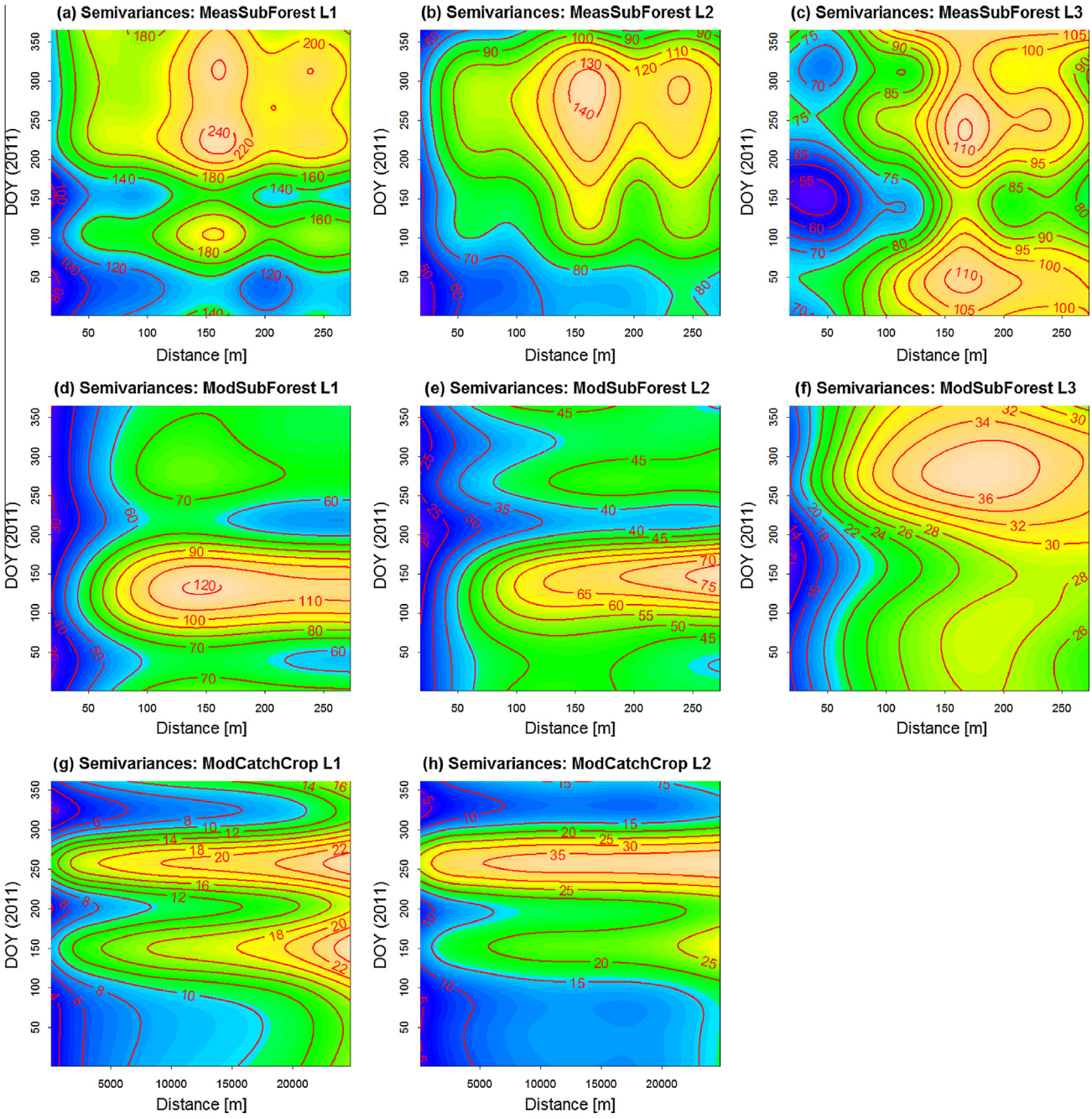

Fig. 7. Contour plot of the semivariance values of different datasets with the distance values on the *x*-axis, the day of year (DOY) on the *y*-axis and the color-coded semivariances. The semivariance-surfaces were interpolated using a smoothing spline algorithm (R library mgcv (Wood, 2006)). Only the datasets with daily data were chosen for the analysis.

all. For the MeasSubForest dataset we could only find stable *D* values at lower distances with an irregular behavior after the scale break (at around 135 m for L1, 170 m for L2 and 200 m for L3). Comparable results could be found for the ModSubForest dataset with scale breaks at around 110 m for L1, 90 m for L2 and 180 m for L3. This tendency of increasing distances of the scale breaks with lower soil layers (with the exception of ModSubForest L2) was also observed for the range values in the semivariance analysis. Again, a larger spatial organization of soil moisture patterns in deeper soil layers for the forest sub-catchment in both datasets was observed, supporting the findings of Manfreda et al. (2007).

The overall high *D* values in our analysis are in good agreement with other studies which found high fractal dimensions for soil parameters (Burrough, 1983), having a strong connections to soil moisture data, but they are not calculated using the variogram method (Kim and Barros, 2002). Many other studies have shown differences in the calculated fractal dimensions with different computational methods (De Jong and Burrough, 1995; Klinkenberg and Goodchild, 1992). In comparison to other methods (e.g., isarithm or triangular prism) the variogram method yields higher fractal dimension estimates in datasets with high variability (Lam et al., 2002), but this does not influence the estimation of scale breaks. The variogram method was used in our analysis, because of its applicability to our datasets, with an irregular grid of data points or regular grids with missing values.

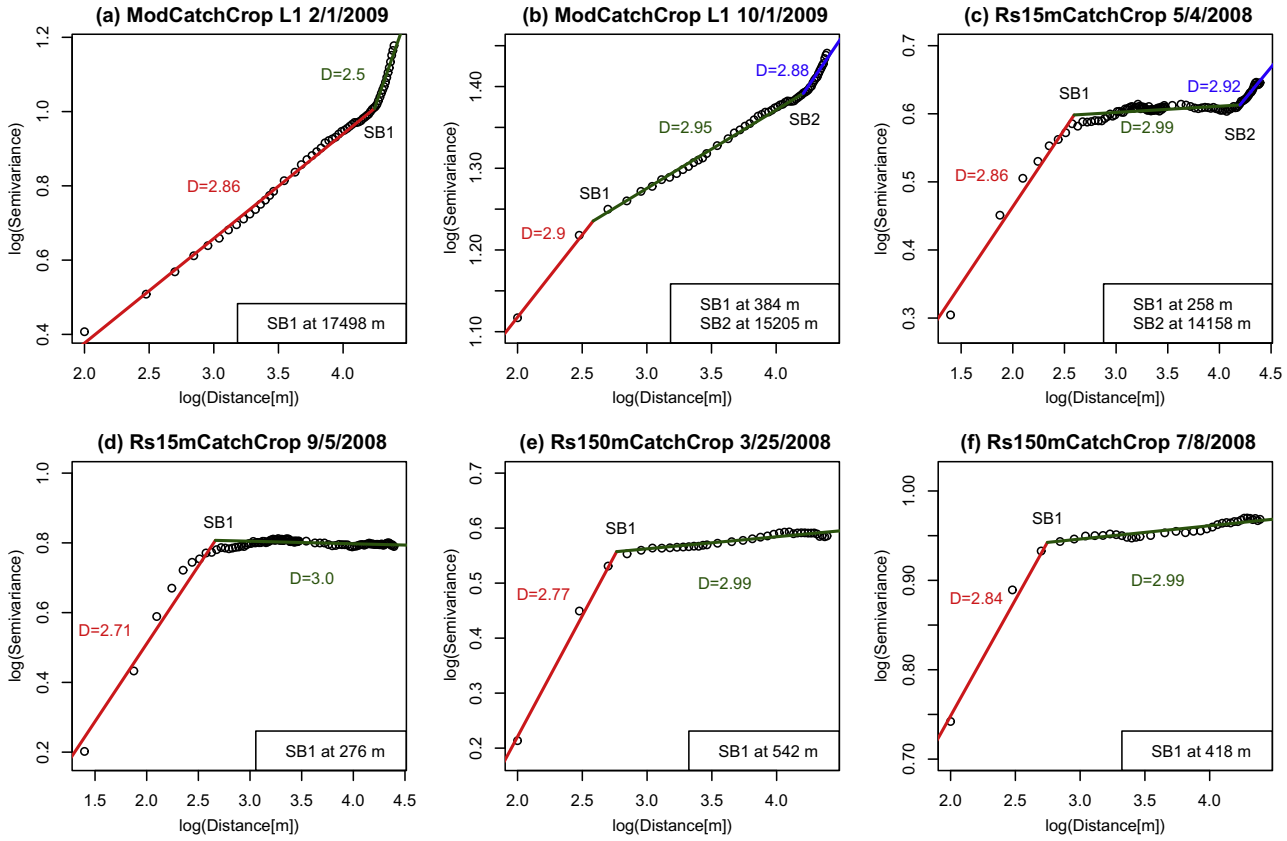

Fig. 8. Log–log plot of the semivariance values of exemplary dates and datasets, regression lines from the segmented regression, the associated fractal dimensions (D), derived from the slope of the regression segments, separated by the scales breaks (SB, with the indication of the distance in the legend).

4. Summary and conclusions

We analyzed the spatial patterns of soil moisture and their temporal development using nine different datasets from measurement, modeling and radar remote sensing within the Rur catchment in Western Germany. The datasets capture soil moisture dynamics on very different spatial and temporal scales (extent, spacing, support) and on different land use – topography – soil combinations. The soil moisture variability as well as the relationship of mean soil moisture, soil moisture variability and autocorrelation structure of the soil moisture patterns were analyzed.

We found very low mean soil moisture values on a plot scale dataset on bare soil resulting from very dry soil moisture conditions at the beginning of the short measurement period (temporal extent) and only small scale variability of soil parameters. The other extreme with high mean soil moisture value and high CV values was found in a small forest sub-catchment caused by higher precipitation values and a heterogeneous topography, which is typical for the mountainous region of the southern part of the Rur catchment. For grassland, the second major land use in the southern part of the catchment, we found high mean soil moisture values comparable to the forest sub catchment, but with much lower SD. The datasets for the northern part of the Rur catchment showed generally lower mean soil moisture values caused by lower precipitation rates. The main reasons for the observed spatial variability in the cropped area with very flat terrain are the influence of vegetation (temporal differences of evapotranspiration rates of the different crops), management (field size, planting dates, harvesting dates) and soil parameters (porosity, field capacity). Generally, smaller CV values for remotely sensed surface soil moisture are linked to the larger spatial support by the sensor, averaging small scale variability. Nevertheless, the CV values of the 15 m remote sensing dataset are comparable to the CV values of the 150 m remote sensing dataset, despite lower mean soil moisture and the smaller spatial support. This might be ascribed to the non-corresponding measuring dates and to the different processing chains and retrieval algorithms for the dual polarimetric L-band sensor and the single polarimetric C-band sensor. The CosmicCatchAll dataset shows high CV values, despite the largest spatial support of all datasets. This high spatial variability can be explained by the choice of the scattered locations of the stations over the drier northern part and wetter southern part, with the purpose to sample some extreme conditions of the whole spectrum of land use – topography – soil combinations within the whole catchment.

For all datasets we found negative correlations between the coefficient of variation and the mean soil moisture, indicating lower spatial variability at higher mean soil moisture values. For the forest sub-catchment compared to the cropped areas, the offset of this relationship was larger, with generally larger CV values at comparable mean soil moisture values. Moreover, a decrease of the spatial variability with decreasing spatial extent and increasing spatial support could be observed within the different datasets. Such a relationship between our datasets cannot be found, because the effect of varying measurement or modeling scale is often masked and superimposed by the larger true variability of the natural processes and parameters within the single datasets.

Using the geostatistical analysis of the soil moisture values it was possible to identify three groups with similar values for sill and range: (i) modeled and measured datasets from the forest sub-catchment with large sill values and small range values, (ii) remotely sensed datasets from the northern part of the Rur catchment with small to medium sill values and medium range values,

and (iii) modeled datasets from the northern part of the Rur catchment with medium sill values and large range values. The small range values in (i) are associated with soil and topographic characteristics of the forest sub catchment, medium range values in (ii) with the land-use structure (field size) of the cropped area and large range values in (iii) with large scale variability of soil parameters between soil types.

All analyzed soil moisture patterns showed a multifractal behavior (only partial self-similarity over limited ranges of scales), with at least one scale break and generally high fractal dimensions. The scale breaks found with the fractal analysis are consistent with the above-mentioned grouped range values (i), (ii) and (iii) originating from the geostatistical analysis. The advantage of the fractal method over the geostatistical method in our analysis was that the maximum range of the analysis does not have to be cut in order to remove nonstationarity at longer ranges and to get a good model fit in the geostatistical analysis. In our datasets, we found stationarity only at some ranges, indicating different sources of spatial variability at different ranges. Including the longer ranges in the fractal analysis, it was even possible to detect two scale breaks (associated with land use structure and soil type) within the datasets with large spatial extent, instead of one with the geostatistical analysis. Thus, a multifractal model is seen as an appropriate approach to capture and describe the nested scales of variation of soil moisture patterns for the largest part of our datasets.

The joined analysis of the different datasets showed that corresponding scale breaks can be found between different datasets and therefore these scale breaks are no artefacts from input data (e.g., from the soil map in the model studies). Particularly for the forest sub-catchment, the results suggest that the model underestimated the small scale complexity of the natural systems and that the small differences in soil moisture dynamic between the datasets, especially at the upper and lower bounds of soil moisture (at maximum porosity and wilting point in the soils) can have a large influence on the soil moisture patterns and their autocorrelation structure. The influence of the vegetation can lead to a decrease or an increase of spatial variability in the soil moisture pattern, depending on the prevalent type of land use. At the forest test site we found a homogenizing effect of the uniform vegetation, contrary to the cropped areas, where the shifted periods of maximum water uptake of the different crops on different fields and the agricultural management (e.g., planting dates, harvesting dates, field sizes) generated an increase of spatial variability in the soil moisture patterns.

Acknowledgements

We gratefully acknowledge financial support by the SFB/TR 32 "*Patterns in Soil-Vegetation-Atmosphere Systems: Monitoring, Modelling, and Data Assimilation*" funded by the German Science Foundation (DFG) and by TERENO "*Terrestrial Environmental Observatories*" funded by the Helmholtz Association and the Federal Ministry of Education and Research (BMBF).

References

Baatz, R., Bogena, H.R., Hendricks Franssen, H.J., Huisman, J.A., Qu, W., Montzka, C., Vereecken, H., 2014. Calibration of a catchment scale cosmic-ray probe network: a comparison of three parameterization methods. J. Hydrol. 516, 231–244.

Barth, M., Hennicker, R., Kraus, A., Ludwig, M., 2004. DANUBIA: an integrative simulation system for global change research in the Upper Danube Basin. Cybernet. Syst. 35 (7–8), 639–666.

Barthel, R., Reichenau, T.G., Krimly, T., Dabbert, S., Schneider, K., Mauser, W., 2012. Integrated modeling of global change impacts on agriculture and groundwater resources. Water Resour. Manage 26 (7), 1929–1951.

Blöschl, G., Sivapalan, M., 1995. Scale issues in hydrological modeling – a review. Hydrol. Process. 9 (3–4), 251–290.

Bogena, H.R., Herbst, M., Huisman, J.A., Rosenbaum, U., Weuthen, A., Vereecken, H., 2010. Potential of wireless sensor networks for measuring soil water content variability. Vadose Zone J. 9 (4), 1002–1013.

Bogena, H.R., Huisman, J.A., Baatz, R., Franssen, H.J.H., Vereecken, H., 2013. Accuracy of the cosmic-ray soil water content probe in humid forest ecosystems: the worst case scenario. Water Resour. Res. 49 (9), 5778–5791.

Burrough, P.A., 1983. Multiscale sources of spatial variation in soil. I. The application of fractal concepts to nested levels of soil variation. J. Soil Sci. 34 (3), 577–597.

Choi, M., Jacobs, J.M., 2007. Soil moisture variability of root zone profiles within SMEX02 remote sensing footprints. Adv. Water Resour. 30 (4), 883–896.

Choi, M., Jacobs, J.M., 2011. Spatial soil moisture scaling structure during Soil Moisture Experiment 2005. Hydrol. Process. 25 (6), 926–932.

Cornelissen, T., Diekkrüger, B., Bogena, H.R., 2014. Significance of scale and lower boundary condition in the 3D simulation of hydrological processes and soil moisture variability in a forested headwater catchment. J. Hydrol. 516, 140–153.

Corradini, C., 2014. Soil moisture in the development of hydrological processes and its determination at different spatial scales. J. Hydrol. 516, 1–5.

De Jong, S., Burrough, P., 1995. A fractal approach to the classification of Mediterranean vegetation types in remotely sensed images. Photogramm. Eng. Remote Sens. 61 (8), 1041–1053.

Desilets, D., Zreda, M., 2013. Footprint diameter for a cosmic-ray soil moisture probe: theory and Monte Carlo simulations. Water Resour. Res. 49 (6), 3566–3575.

Desilets, D., Zreda, M., Ferré, T.P.A., 2010. Nature's neutron probe: land surface hydrology at an elusive scale with Cosmic Rays. Water Resour. Res. 46 (11), W11505.

Diggle, P., Ribeiro, P.J., 2007. Model-based Geostatistics. Springer Series in Statistics. Springer, New York, NY, xiii, 228p.

Famiglietti, J.S., Rudnicki, J.W., Rodell, M., 1998. Variability in surface moisture content along a hillslope transect: Rattlesnake Hill, Texas. J. Hydrol. 210 (1–4), 259–281.

Famiglietti, J.S., Devereaux, J.A., Laymon, C.A., Tsegaye, T., Houser, P.R., Jackson, T.J., Graham, S.T., Rodell, M., van Oevelen, P.J., 1999. Ground-based investigation of soil moisture variability within remote sensing footprints during the Southern Great Plains 1997 (SGP97) Hydrology Experiment. Water Resour. Res. 35 (6), 1839–1851.

Famiglietti, J.S., Ryu, D., Berg, A.A., Rodell, M., Jackson, T.J., 2008. Field observations of soil moisture variability across scales. Water Resour. Res. 44 (1), W01423.

Gao, J., Xia, Z.-G., 1996. Fractals in physical geography. Prog. Phys. Geogr. 20 (2), 178–191.

Goderniaux, P., Brouyere, S., Fowler, H.J., Blenkinsop, S., Therrien, R., Orban, P., Dassargues, A., 2009. Large scale surface–subsurface hydrological model to assess climate change impacts on groundwater reserves. J. Hydrol. 373 (1–2), 122–138.

Goodchild, M.F., Mark, D.M., 1987. The fractal nature of geographic phenomena. Ann. Assoc. Am. Geogr. 77 (2), 265–278.

Grant, L., Seyfried, M., McNamara, J., 2004. Spatial variation and temporal stability of soil water in a snow-dominated, mountain catchment. Hydrol. Process. 18 (18), 3493–3511.

Grayson, R., Blöschl, G., 2000. Spatial Patterns in Catchment Hydrology: Observations and Modelling. Cambridge University Press, New York, 404 pp.

Grayson, R.B., Western, A.W., Chiew, F.H.S., Blöschl, G., 1997. Preferred states in spatial soil moisture patterns: local and nonlocal controls. Water Resour. Res. 33 (12), 2897–2908.

Green, T.R., Erskine, R.H., 2004. Measurement, scaling, and topographic analyses of spatial crop yield and soil water content. Hydrol. Process. 18 (8), 1447–1465.

Hawley, M.E., Jackson, T.J., McCuen, R.H., 1983. Surface soil moisture variation on small agricultural watersheds. J. Hydrol. 62 (1–4), 179–200.

Hebrard, O., Voltz, M., Andrieux, P., Moussa, R., 2006. Spatio-temporal distribution of soil surface moisture in a heterogeneously farmed Mediterranean catchment. J. Hydrol. 329 (1–2), 110–121.

Herbst, M., Diekkruger, B., 2003. Modelling the spatial variability of soil moisture in a micro-scale catchment and comparison with field data using geostatistics. Phys. Chem. Earth 28 (6–7), 239–245.

Herbst, M., Prolingheuer, N., Graf, A., Huisman, J.A., Weihermuller, L., Vanderborght, J., 2009. Characterization and understanding of bare soil respiration spatial variability at plot scale. Vadose Zone J. 8 (3), 762–771.

Hu, W., Shao, M.A., Wang, Q.J., Reichardt, K., 2008. Soil water content temporal–spatial variability of the surface layer of a Loess Plateau hillside in China. Scientia Agricola 65, 277–289.

Hu, W., Shao, M.G., Han, F.P., Reichardt, K., 2011. Spatio-temporal variability behavior of land surface soil water content in shrub- and grass-land. Geoderma 162 (3–4), 260–272.

Kim, G., Barros, A.P., 2002. Space–time characterization of soil moisture from passive microwave remotely sensed imagery and ancillary data. Remote Sens. Environ. 81 (2–3), 393–403.

Klinkenberg, B., Goodchild, M.F., 1992. The fractal properties of topography: a comparison of methods. Earth Surf. Proc. Land. 17 (3), 217–234.

Korres, W., Koyama, C.N., Fiener, P., Schneider, K., 2010. Analysis of surface soil moisture patterns in agricultural landscapes using Empirical Orthogonal Functions. Hydrol. Earth Syst. Sci. 14 (5), 751–764.

Korres, W., Reichenau, T.G., Schneider, K., 2013. Patterns and scaling properties of surface soil moisture in an agricultural landscape: an ecohydrological modeling study. J. Hydrol. 498, 89–102.

Koyama, C.N., Schneider, K., 2014. Biomass-corrected quantitative soil moisture estimation from dual polarimetric ALOS PALSAR data. Ieee Trans. Geosci. Remote Sens., in review.

Koyama, C.N., Korres, W., Fiener, P., Schneider, K., 2010. Variability of surface soil moisture observed from multitemporal C-Band synthetic aperture radar and field data. Vadose Zone J. 9 (4), 1014–1024.
Lam, N.S.-N., Qiu, H.-L., Quattrochi, D.A., Emerson, C.W., 2002. An evaluation of fractal methods for characterizing image complexity. Cartogr. Geogr. Inform. Sci. 29 (1), 25–35.
Lawrence, J.E., Hornberger, G.M., 2007. Soil moisture variability across climate zones. Geophys. Res. Lett. 34 (20), L20402.
Loew, A., Ludwig, R., Mauser, W., 2006. Derivation of surface soil moisture from ENVISAT ASAR wide swath and image mode data in agricultural areas. IEEE Trans. Geosci. Remote Sens. 44 (4), 889–899.
Mandelbrot, B.B., 1977. Fractals: Form, Chance and Dimension. Freeman, San Francisco, 365 pp.
Manfreda, S., McCabe, M.F., Fiorentino, M., Rodríguez-Iturbe, I., Wood, E.F., 2007. Scaling characteristics of spatial patterns of soil moisture from distributed modelling. Adv. Water Resour. 30 (10), 2145–2150.
Mark, D., Aronson, P., 1984. Scale-dependent fractal dimensions of topographic surfaces: an empirical investigation, with applications in geomorphology and computer mapping. J. Int. Assoc. Math. Geol. 16 (7), 671–683.
Montzka, C., Bogena, H.R., Weihermuller, L., Jonard, F., Bouzinac, C., Kainulainen, J., Balling, J.E., Loew, A., Dall'Amico, J.T., Rouhe, E., Vanderborght, J., Vereecken, H., 2013. Brightness temperature and soil moisture validation at different scales during the SMOS validation campaign in the Rur and Erft catchments, Germany. IEEE Trans. Geosci. Remote Sens. 51 (3), 1728–1743.
Muggeo, V.M.R., 2003. Estimating regression models with unknown break-points. Stat. Med. 22 (19), 3055–3071.
Oliver, M.A., Webster, R., 1987. The elucidation of soil pattern in the Wyre Forest of the West-Midlands, England. 1. Multivariate distribution. J. Soil Sci. 38 (2), 279–291.
Pan, F., Peters-Lidard, C.D., 2008. On the relationship between mean and variance of soil moisture fields. J. Am. Water Resour. Assoc. 44 (1), 235–242.
Panday, S., Huyakorn, P.S., 2004. A fully coupled physically-based spatially-distributed model for evaluating surface/subsurface flow. Adv. Water Resour. 27 (4), 361–382.
Peters-Lidard, C.D., Pan, F., Wood, E.F., 2001. A re-examination of modeled and measured soil moisture spatial variability and its implications for land surface modeling. Adv. Water Resour. 24 (9–10), 1069–1083.
R Core Team, 2014. R: A Language and Environment For statistical Computing. R Foundation for Statistical Computing, Vienna, Austria.
Reynolds, S.G., 1970. The gravimetric method of soil moisture determination Part III An examination of factors influencing soil moisture variability. J. Hydrol. 11 (3), 288–300.
Richter, F., 2008. Bodenkarte zur Standorterkundung. Verfahren Quellgebiet Wüstebachtal (Forst). Geologischer Dienst Nordrhein-Westfalen, Krefeld, Germany.
Rodriguez-Iturbe, I., Vogel, G.K., Rigon, R., Entekhabi, D., Castelli, F., Rinaldo, A., 1995. On the spatial-organization of soil moisture fields. Geophys. Res. Lett. 22 (20), 2757–2760.
Rodriguez-Iturbe, I., Isham, V., Cox, D.R., Manfreda, S., Porporato, A., 2006. Space–time modeling of soil moisture: stochastic rainfall forcing with heterogeneous vegetation. Water Resour. Res. 42 (6), W06D05.
Rombach, M., Mauser, W., 1997. Multi-annual analysis of ERS surface soil moisture measurements of different land uses, Proc. 3rd ERS Scientific Symposium. Eur. Space Agency, Florence, pp. 703–708.
Rosenbaum, U., Bogena, H.R., Herbst, M., Huisman, J.A., Peterson, T.J., Weuthen, A., Western, A.W., Vereecken, H., 2012. Seasonal and event dynamics of spatial soil moisture patterns at the small catchment scale. Water Resour. Res. 48 (10), W10544.
Ryu, D., Famiglietti, J.S., 2005. Characterization of footprint-scale surface soil moisture variability using Gaussian and beta distribution functions during the Southern Great Plains 1997 (SGP97) hydrology experiment. Water Resour. Res. 41 (12), W12433.
Sun, W., Xu, G., Gong, P., Liang, S., 2006. Fractal analysis of remotely sensed images: a review of methods and applications. Int. J. Remote Sens. 27 (22), 4963–4990.
Svetlitchnyi, A.A., Plotnitskiy, S.V., Stepovaya, O.Y., 2003. Spatial distribution of soil moisture content within catchments and its modelling on the basis of topographic data. J. Hydrol. 277 (1–2), 50–60.
Teuling, A.J., Troch, P.A., 2005. Improved understanding of soil moisture variability dynamics. Geophys. Res. Lett. 32 (5), L05404.
Vereecken, H., Kamai, T., Harter, T., Kasteel, R., Hopmans, J., Vanderborght, J., 2007. Explaining soil moisture variability as a function of mean soil moisture: a stochastic unsaturated flow perspective. Geophys. Res. Lett. 34 (22), L22402.
Vereecken, H., Kollet, S., Simmer, C., 2010. Patterns in soil–vegetation–atmosphere systems: monitoring, modeling, and data assimilation. Vadose Zone J. 9 (4), 821–827.
Waldhoff, G., 2010. Land use classification of 2009 for the Rur catchment.
Western, A.W., Blöschl, G., 1999. On the spatial scaling of soil moisture. J. Hydrol. 217 (3–4), 203–224.
Western, A.W., Grayson, R.B., 1998. The Tarrawarra data set: soil moisture patterns, soil characteristics, and hydrological flux measurements. Water Resour. Res. 34 (10), 2765–2768.
Western, A.W., Blöschl, G., Grayson, R.B., 1998. Geostatistical characterisation of soil moisture patterns in the Tarrawarra a catchment. J. Hydrol. 205 (1–2), 20–37.
Western, A.W., Grayson, R.B., Blöschl, G., Willgoose, G.R., McMahon, T.A., 1999a. Observed spatial organization of soil moisture and its relation to terrain indices. Water Resour. Res. 35 (3), 797–810.
Western, A.W., Grayson, R.B., Green, T.R., 1999b. The Tarrawarra project: high resolution spatial measurement, modelling and analysis of soil moisture and hydrological response. Hydrol. Process. 13 (5), 633–652.
Western, A.W., Zhou, S.L., Grayson, R.B., McMahon, T.A., Blöschl, G., Wilson, D.J., 2004. Spatial correlation of soil moisture in small catchments and its relationship to dominant spatial hydrological processes. J. Hydrol. 286 (1–4), 113–134.
Wood, S.N., 2006. Generalized Additive Models: an Introduction with R. Texts in Statistical Science. Chapman & Hall/CRC, Boca Raton, FL, xvii, 391p.
Yoo, C., Kim, S., 2004. EOF analysis of surface soil moisture field variability. Adv. Water Resour. 27 (8), 831–842.
Zacharias, S., Bogena, H., Samaniego, L., Mauder, M., Fuß, R., Pütz, T., Frenzel, M., Schwank, M., Baessler, C., Butterbach-Bahl, K., Bens, O., Borg, E., Brauer, A., Dietrich, P., Hajnsek, I., Helle, G., Kiese, R., Kunstmann, H., Klotz, S., Munch, J.C., Papen, H., Priesack, E., Schmid, H.P., Steinbrecher, R., Rosenbaum, U., Teutsch, G., Vereecken, H., 2011. A network of terrestrial environmental observatories in German. Vadose Zone J. 10 (3), 955–973.
Zreda, M., Desilets, D., Ferre, T.P.A., Scott, R.L., 2008. Measuring soil moisture content non-invasively at intermediate spatial scale using cosmic-ray neutrons. Geophys. Res. Lett. 35 (21), L21402.
Zucco, G., Brocca, L., Moramarco, T., Morbidelli, R., 2014. Influence of land use on soil moisture spatial–temporal variability and monitoring. J. Hydrol. 516, 193–199.